

Original Article

Cite this article: Tee JB, Dnyanmote AV, Lorenzo MK, Lee OR, Grisaru S, Suk M, and Acott PD (2020) Pkd1-targeted mutation reveals a role for the Wolffian duct in autosomal dominant polycystic kidney disease. *Journal of Developmental Origins of Health and Disease* **11**: 78–85. <https://doi.org/10.1017/S2040174419000436>

Received: 19 February 2019
Revised: 21 May 2019
Accepted: 17 June 2019
First published online: 15 August 2019

Keywords:

Polycystic kidney; Wolffian duct; kidney development; Pkd1; microRNAs

Address for correspondence:

J. B. Tee, Department of Pediatrics, IWK Health Centre – Dalhousie University, 5850 University Ave, Halifax, NS, Canada.
Email: james.tee@iwk.nshealth.ca

Pkd1-targeted mutation reveals a role for the Wolffian duct in autosomal dominant polycystic kidney disease

J. B. Tee¹, A. V. Dnyanmote¹, M. K. Lorenzo², O. R. Lee³, S. Grisaru⁴, M. Suk³ and P. D. Acott¹

¹Department of Pediatrics, IWK Health Centre – Dalhousie University, 5850 University Ave, Halifax, NS, B3K 6R8, Canada; ²Department of Pediatrics, Hospital for Sick Children – University of Toronto, 555 University Ave, Toronto, ON, M5G 1X8 Canada; ³Department of Family Medicine, University of Alberta, 8215 - 112 St., Edmonton, AB, T6G 2R3 Canada and ⁴Department of Pediatrics, Alberta Children's Hospital – University of Calgary, 2888 Shaganappi Trail NW, Calgary, AB, T3B 6A9 Canada

Abstract

Several life-threatening diseases of the kidney have their origins in mutational events that occur during embryonic development. In this study, we investigate the role of the Wolffian duct (WD), the earliest embryonic epithelial progenitor of renal tubules, in the etiology of autosomal dominant polycystic kidney disease (ADPKD). ADPKD is associated with a germline mutation of one of the two Pkd1 alleles. For the disease to occur, a second event that disrupts the expression of the other inherited Pkd1 allele must occur. We postulated that this secondary event can occur in the pronephric WD. Using Cre-Lox recombination, mice with WD-specific deletion of one or both Pkd1 alleles were generated. Homozygous Pkd1-targeted deletion in WD-derived tissues resulted in mice with large cystic kidneys and serologic evidence of renal failure. In contrast, heterozygous deletion of Pkd1 in the WD led to kidneys that were phenotypically indistinguishable from control in the early postnatal period. High-throughput sequencing, however, revealed underlying gene and microRNA (miRNA) changes in these heterozygous mutant kidneys that suggest a strong predisposition toward developing ADPKD. Bioinformatic analysis of this data demonstrated an upregulation of several miRNAs that have been previously associated with PKD; pathway analysis further demonstrated that the differentially expressed genes in the heterozygous mutant kidneys were over-represented in signaling pathways associated with maintenance and function of the renal tubular epithelium. These results suggest that the WD may be an early epithelial target for the genetic or molecular signals that can lead to cyst formation in ADPKD.

Introduction

Autosomal dominant polycystic kidney disease (ADPKD) is characterized by the development of multiple fluid-filled epithelial-derived cysts. It is the most commonly inherited disorder of the kidneys, affecting 1 in every 500 people, and is the leading genetic cause of end-stage renal disease^{1,2}. A growing number of children are now being diagnosed with ADPKD due in part to advances in fetal ultrasonography, with nearly 20% of pediatric cases being detected *in utero*³. The most common form of this disease is type 1 ADPKD, which accounts for 85% of cases and is caused by the germline mutation of one of the two alleles of Pkd1^{4,5}. A loss of expression of the Pkd1 gene, located on chromosome-17 in mice and -16 in humans, leads to a decrease in its encoded glycoprotein, polycystin-1⁶, an essential structural component of the primary cilia lining the luminal surface of the renal tubule that serves to maintain its integrity^{7–11}. A complete loss of heterozygosity at the functional Pkd1 locus occurs in only a minority of cysts^{12–15}. By contrast, polycystin-1 continues to be expressed in the epithelial cells of the majority (~80%) of cysts in humans with type 1 ADPKD, suggesting that a regulatory factor that affects the expression level of the second allele exists to ultimately activate cystogenesis¹⁶. Evidence from the analysis of cystic epithelia from animal models and humans with ADPKD indicates that such a “secondary event” might predispose the tubular epithelium to undergo cystogenesis through the disruption or insufficient expression of the inherited normal Pkd1 allele. Moreover, the detection of renal cysts in some embryos suggests that regulatory signaling activity underlying these secondary cyst-inducing events can indeed occur early on in kidney development. However, the provenance of these regulatory factors and the time point during renal embryogenesis at which these signals might first originate remains less clearly understood³. Gene expression patterns or molecular signaling underlying these secondary cellular events of cystogenesis, particularly increased proliferation rates, have been found even in non-cystic tubular epithelium in ADPKD. This suggests that regulatory signals compromising tubular architecture are likely to predate cystogenesis and are perhaps activated during renal organogenesis¹⁷. One such regulatory factor that has been suggested is the microRNA (miRNA), a class of functional,

non-translated small ribonucleic acid molecules that have drawn increasing attention for their role in regulating cellular processes^{18–20}. MiRNAs regulate gene expression at the posttranscriptional level by base-pairing with the 3' UTR of the target gene, causing cleavage or degradation of the cognate mRNA or by preventing translation initiation. Furthermore, the potential for miRNAs to play a post-transcriptional regulatory role in modifying the expression of Pkd1 is supported by the existence of predicted binding sites on the Pkd1 transcript for several miRNAs, the development of renal cysts observed with the embryonic removal of Dicer (an enzyme required for the processing of most miRNAs), as well as with the generation of artificial miRNAs against the Pkd1 gene^{21–25}.

Mice strains that feature targeted homozygous mutations of Pkd1 (including those created by deletion or insertion of a stop codon into the gene) invariably feature embryonic lethality as early as embryonic day E13.5 of a mouse's 21-day gestational period, thereby limiting their utility in studying the progression of ADPKD through the stages of renal tubular development^{26–30}. Nevertheless, the late onset of detectable cysts, as is often seen in heterozygous models of type 1 ADPKD, is compatible with the possibility of secondary events during early embryonic development that could potentially initiate a progression toward cyst formation. Thus, in order to evaluate the earliest embryonic time point at which these secondary events may originate in ADPKD, we selectively targeted the Pkd1 gene in the Wolffian duct (WD), the earliest structure of kidney development. The WD, through a process of bud formation, elongation, and branching, gives rise to the collecting ducts of the distal nephron in which cysts in ADPKD can be found³¹. Pkd1 is normally expressed in the epithelial cells of the WD making this early renal structure a potential source for the regulatory signals that govern this unknown secondary cystogenic event³². Limiting the Pkd1 mutation to the WD, therefore, allowed for the focused examination of developmentally critical gene expression in the earliest structures of renal tubular development without genetic interference from other systems such as the liver and spleen that are also known to be affected in ADPKD.

Materials and methods

Mouse strains and Pkd1-targeted knockdown in the WD

A congenic knockout mouse strain Pkd1tm2Ggg possessing loxP sites flanking exons 2–4 of Pkd1 (Pkd1^{fllox/fllox}; Jackson Laboratories, Bar Harbor, ME) was crossbred with a transgenic mouse strain Hoxb7-Cre13Amc (Hoxb7-Cre; Jackson Laboratories, Bar Harbor, ME) in which Cre recombinase enzyme is expressed in only the WD and WD-derived structures (with minimal expression in the dorsal root ganglia and the spinal cord) under the control of the mouse homeobox B7 enhancer and promoter^{17,30,33–35}. Both strains feature the same C57BL/6 genetic background and were bred for 10 generations to establish their respective colonies. The Cre recombinase in the resulting offspring catalyzes recombination between the flanking loxP sites to produce a heterozygous WD-specific deletion of one of the two Pkd1 alleles (Pkd1^{+/-}; Hoxb7-Cre). Homozygous WD-specific deletion of the Pkd1 alleles was achieved by crossing two of these heterozygous mice. Offspring that were not carriers for Hoxb7-Cre and thus lacked Cre recombinase deletion of Pkd1 served as the control group.

Genotyping

Genomic DNA was extracted from individual mice samples using E.Z.N.A. Tissue DNA Kit (OmegaBiotek). The DNA was then

combined with Red Extract-N-Amp PCR reaction mix (Sigma) and primers to create a final volume of 20 µl for PCR amplification. The set of primers used to identify the presence of the mutant floxed Pkd1 gene were (forward) 5'-CCTGCCTTGCTCTACTTTCC-3' and (reverse) 5'-AGGGCTTTTCTTGCTGGTCT-3'. The set of primers used to identify the presence of the Hoxb7-Cre transgene were (forward) 5'-GGTCACGTGGTCAGAGAGG-3' and (reverse) 5'-CTCATCACTCGTTGCATCGA-3', which were run concurrently with internal positive control primers (forward) 5'-CAAATGTTGCTTGCTGGTG-3' and 5'-GTCAGTCGAGTGCACAGTTT-3'. The PCR was performed at 94°C, 30 s; 55°C, 1 min; 72°C, 1 min for 35 cycles, and the amplification products were then separated on a 1.5% agarose gel. A homozygous floxed Pkd1 gene was identifiable by a 250-bp band; heterozygous by both 250 and 132 bp bands; and the absence of any loxP-flanked gene by only 132 bp bands. The Hoxb7-Cre transgene was identifiable by the presence of 300 bp bands with the internal positive control providing a 200-bp band.

Clinical chemistry

Mice were euthanized and 55 µl of undiluted serum was immediately taken and submitted to Charles River Laboratories (Wilmington, MA) for the measurement of creatinine levels. The colorimetric serum creatinine assay utilized an Ace Alera chemistry analyzer with Alfa Wassermann reagents based on a modification of the Jaffe reaction.

Histology

Extracted kidneys were fixed in 10% formalin overnight and then paraffinized. Sagittal tissue sections of 5 µm thickness were taken and stained with hematoxylin and eosin (H&E).

Sequencing and microarray analysis

Kidney samples were transferred into RNALater (Ambion, Carlsbad, CA) immediately after the extraction to prevent RNA degradation. For each condition, biological triplicate samples of total RNA were extracted from nine kidneys (three kidneys per sample) using Ambion's mirVana miRNA Isolation Kit (Carlsbad, CA). Gene expression profiles were generated concurrently from each sample source as follows: RNA-Seq and high-throughput sequencing were performed on the same sample source on a 5500 SOLiD sequencer (Applied Biosystems, Carlsbad, CA) at the University of Calgary for the quantitation of gene and miRNA expression, respectively. RNA-Seq expression values were normalized as reads per kilo base of exon model per one million mapped reads (RPKM)^{36–38}. Expression sequencing reads of poor quality as indicated by a Phred score <20 (equivalent to 99% of base call accuracy) were excluded. Validation of gene expression results was performed by microarray profiling of the biological triplicate samples, each with a minimum RNA amount of 2 µg and concentration of 200 ng/µl, using Affymetrix's Whole Transcriptome 1.0ST Mouse Array Genechip (Santa Clara, CA) at the University of Calgary's Microarray Facility. Results were analyzed using Partek Genomics Suite (Partek, St. Louis, MO). Alignment of sequencing data was performed against mouse genome annotation dataset NCBI37/mm9 (University of California Santa Cruz, CA). Hierarchical clustering was performed in Partek Genomics Suite with standardization based on shifting gene expression to mean of 0 and scaling to standard deviation of 1. Pathway analysis on the differentially expressed significant genes was carried out using Reactome, a publically available online

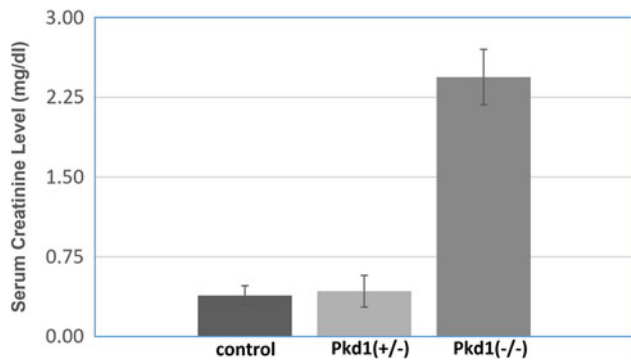


Fig. 1. Renal failure with targeted deletion of Pkd1 in the WD. Serum creatinine levels taken at postpartum day 14. The homozygous Pkd1^{-/-}; Hoxb7-Cre mouse had significant elevation of serum creatinine compared to the heterozygous Pkd1^{+/-}; Hoxb7-Cre mouse and control (Pkd1^{+/+}) mouse.

bioinformatics tool³⁹. The miRNA associated with differentially expressed significant genes was identified using miRNet (<http://www.mirnet.ca>), a web-based tool for studying biological function and regulatory mechanisms of miRNA through network-based statistical analysis and visualization approaches⁴⁰. Network visualization and analyses were conducted using Cytoscape. All expression data were uploaded into NCBI's Gene Expression Omnibus.

Animal care

The care and use of animals described in this study conform to the procedures of the laboratory's Animal Protocol M09133 and were approved by the Animal Care Committee of the University of Calgary.

Results

Phenotypic characterization of Pkd1-targeted knockdown in the WD

Three groups of mice were generated from the crossing of the congenic knockout mouse strain for Pkd1 and Hoxb7-Cre carrier strains: mice with a WD-specific homozygous deletion of the Pkd1 gene (Pkd1^{-/-}), those with a heterozygous deletion (Pkd1^{+/-}), and control mice that did not carry the deletion (Pkd1^{+/+}). Pkd1^{-/-} mice died at an average of 18 days postpartum ($n = 10$). Terminal blood chemistry performed at 2 weeks of age revealed significant renal failure as manifested by a significant elevation in serum creatinine in the homozygous mice compared to heterozygous and control mice (2.44 ± 0.26SD mg/dl vs. 0.43 ± 0.15 and 0.39 ± 0.09 mg/dl, respectively; Fig. 1). Gross visualization of the kidneys at the time of death in all homozygous mice revealed bilaterally enlarged pale kidneys with large cysts on H&E stain. In contrast, heterozygous mice euthanized at the same age had kidneys that were phenotypically indistinguishable from control kidneys, with no evidence of renal cyst formation (Fig. 2). By 8 weeks of age, 20% of heterozygous mice had developed cysts ($n = 10$). These results demonstrated, for the first time, that suppression of the Pkd1 gene in the WD and WD-derived structures alone can lead to renal cyst formation.

Genotypic characterization of the heterozygous Pkd1(+/-); Hoxb7-Cre kidney

Type 1 ADPKD individuals are constitutionally heterozygous for a Pkd1 mutation, and early embryonic factors regulating initial cyst formation may occur long before slower-growing cysts can be visualized. It was also surmised that the immense phenotypic differences between the sparse tissue of the failing cystic Pkd1^{-/-} kidney versus the control and heterozygote kidneys would very likely conceal subtle differences in genetic expression directly related to cyst growth due to unrelated large changes in RNA and RNA degradation. Therefore, we focused the evaluation on whether the phenotypically normal looking kidneys of the Pkd1(+/-); Hoxb7-Cre heterozygous mouse have an underlying genetic expression profile that was different from the control kidneys^{41,42}. RNA-Seq high-throughput sequencing for gene expression yielded a minimum 73 million alignments per sample and was followed by microarray validation of biological triplicate kidney samples. Two hundred and sixty-seven genes exhibited a greater than twofold difference in expression ($p < 0.05$), and hierarchical clustering confirmed that the control and heterozygous groups cluster in genetically distinct groups (Fig. 3).

Pathway analysis

Pathway analysis was conducted using Reactome, a curated pathway database that can be used for interpretation and analysis of pathway knowledge in the context of human systems biology. Reactome generates this analysis by producing a probability score, which is then corrected for false discovery rate. Reactome analysis of the dataset of significant differentially expressed genes (entities) in the heterozygous mutant kidneys compared to control kidneys that resulted in 25 top pathways that were statistically enriched (overrepresented) is listed in Table 1. The analysis also displayed "reactions" which were defined by Reactome as any biological event that changes the state of a biological molecule. These events can include binding, activation, translocation, degradation, and classical biochemical reactions. Almost all of the pathways that were ranked in this analysis were associated with tubular function, metabolism, and transport activity. Glucuronidation, which is the major pathway involved in phase II metabolism and drug conjugation, ranked the highest. Other notable pathways include biological oxidations involved in biotransformation reactions and xenobiotic metabolism, CYP2E1, glutathione conjugation, and the cytochrome P450 isozyme system. Associated pathways involved in tubular function included peroxisomal protein import and the organic anion transporter system, which is well characterized in the renal tubular epithelium. In addition, pathways involved in fatty acid metabolism and cellular energetics were also highlighted in the analysis.

Prediction of miRNA implicated in PKD

Given the potential role that miRNAs may contribute to cyst formation in ADPKD, we evaluated miRNA associated with mRNA transcripts representing the 267 significantly expressed genes that changed more than twofold in the PKD(+/-) kidneys. This was accomplished using miRNET, a web-based tool to conduct statistical, visual, and network-based analysis of miRNAs functions and

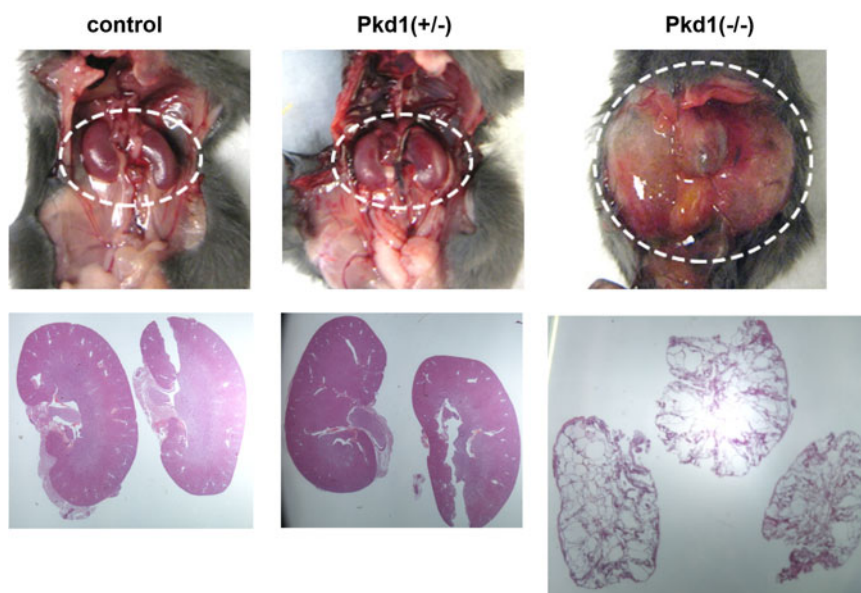


Fig. 2. Cystic phenotype with targeted deletion of *Pkd1* in the WD. *Pkd1*^{-/-}; *Hoxb7*-Cre mice at postpartum day 18 exhibited massively cystic kidneys, visible under both gross examination (top figures) and H&E stains (bottom figures). Kidneys in the heterozygous *Pkd1*^{+/-}; *Hoxb7*-Cre and *Pkd1*^{+/+} control mice were not phenotypically different. Kidneys marked within dashed lines.

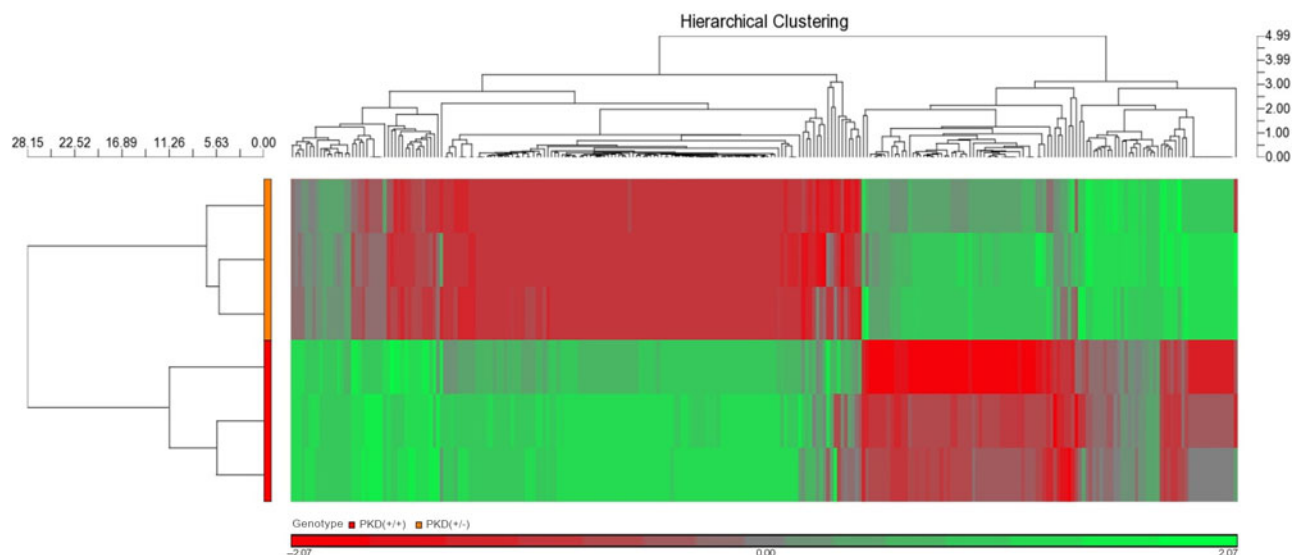


Fig. 3. Distinct hierarchical clustering of gene expression in the *Pkd1*^{+/-}; *Hoxb7*-Cre kidney. Analysis of the gene expression profile between the control (*Pkd1*^{+/+}) and heterozygous (*Pkd1*^{+/-}; *Hoxb7*-Cre) kidney revealed 267 differentially expressed genes (minimum twofold change, one-way ANOVA, *p*-value, and FDR <0.05). Hierarchical clustering of this subset of genes confirmed that the control and heterozygous groups cluster in genetically distinct groups. Kidneys were extracted at postnatal day 18. Samples in cluster tree on left are orange for heterozygous samples and red for control samples. Cluster map color indicates expression of the heterozygous kidney relative to the control kidney with red indicating relative downregulation and green indicating relative upregulation.

their regulatory mechanisms. This tool enables predicting, building, and analyzing networks of miRNA from a starting list of genes of interest. The 267 genes (represented by 245 unique transcript IDs) that were significantly altered in PKD(+/-) kidneys generated a network comprising of 138 nodes that represented 107 miRNAs and their targets, which included 31 genes from the input list. These nodes were connected together with 126 edges that represent biological interactions. As part of its mapping and network creation process, miRNet generated 13 subnetworks of gene-miRNA interactions. We focused on the largest network, which consisted of 78 nodes, 83 edges, and included 13 of the input genes that significantly changed in the PKD(+/-) samples. Several of the predicted miRNA targeting the input genes were found to be associated with PKD as reported in the Mammal ncRNA-Disease

Repository (MNDR v2.0)^{43,44}. The miRNet tool also integrates with Reactome to conduct pathway analysis on specific subnetwork. When this was done for the largest network, the most significant biological function that was identified through the software's hypergeometric filter was organic anion transporters. Network analysis using Cytoscape revealed several genes and miRNAs with potential biologically significant role in orchestrating the signaling underlying cystogenesis (Fig. 4).

Discussion

This study demonstrated that targeted deletion of *Pkd1* in the WD, the embryonic epithelial progenitor of the mammalian kidney, is sufficient to lead to renal cyst formation. This novel finding

Table 1. Overrepresentation (enrichment) pathway analysis in the heterozygous mutant kidneys

Pathway name	Entities (genes)					Reactions (interactions)		
	Found	Total	Ratio	p-value	FDR	Found	Total	Ratio
Glucuronidation	3	55	0.003965679	0.00708247	0.574567395	1	9	7.73E-04
Erythrocytes take up oxygen and release carbon dioxide	2	16	0.001153652	0.00915235	0.574567395	1	6	5.15E-04
Biological oxidations	10	547	0.039440479	0.01538359	0.574567395	26	186	0.015975264
Erythrocytes take up carbon dioxide and release oxygen	2	23	0.001658375	0.01577856	0.574567395	2	7	6.01E-04
O ₂ /CO ₂ exchange in erythrocytes	2	23	0.001658375	0.01577856	0.574567395	3	13	0.001116551
CYP2E1 reactions	2	30	0.002163098	0.01795523	0.574567395	6	6	5.15E-04
Glutathione conjugation	3	67	0.004830918	0.02654923	0.716829089	3	14	0.001202439
Phase II – Conjugation of compounds	6	258	0.018602639	0.02992542	0.718209974	4	70	0.006012196
Tryptophan catabolism	2	48	0.003460956	0.04571801	0.75359957	2	16	0.001374216
Histidine, lysine, phenylalanine, tyrosine, proline, and tryptophan catabolism	4	137	0.009878146	0.04784738	0.75359957	6	53	0.004552091
Methylation of MeSeH for excretion	1	6	4.33E-04	0.06552751	0.75359957	1	2	1.72E-04
Xenobiotics	2	74	0.005335641	0.09238699	0.75359957	15	22	0.001889547
HDMS demethylate histones	2	32	0.002307304	0.11592247	0.75359957	4	17	0.001460105
Biosynthesis of maresin-like SPMs	1	21	0.001514168	0.13269562	0.75359957	3	7	6.01E-04
Fatty acid metabolism	7	429	0.030932295	0.16792776	0.75359957	11	217	0.018637808
Cytochrome P450 – arranged by substrate type	3	186	0.013411205	0.17791574	0.75359957	20	62	0.005325088
Fatty acids	1	29	0.002090994	0.17851508	0.75359957	2	4	3.44E-04
Eicosanoids	1	25	0.001802581	0.17851508	0.75359957	2	6	5.15E-04
Peroxisomal protein import	2	67	0.004830918	0.18107588	0.75359957	3	26	0.002233101
Miscellaneous substrates	1	27	0.001946788	0.18407096	0.75359957	1	5	4.29E-04
Transport of organic anions	1	28	0.002018891	0.18407096	0.75359957	1	8	6.87E-04
Organic anion transporters	1	25	0.001802581	0.20592411	0.75359957	2	9	7.73E-04
Recycling of eIF2:GDP	1	10	7.21E-04	0.21663191	0.75359957	2	2	1.72E-04
NTRK3 as a dependence receptor	0	3	2.16E-04	0.21663191	0.75359957	1	4	3.44E-04

The top 25 significant pathways that were enriched from the subset of genes that were significantly differentially expressed between the heterozygous and control kidneys are listed. Probability scores for pathway enrichment were corrected for false discovery rate using the Benjamini–Hochberg method. All mouse identifiers were converted to their human equivalent.

suggests that the genetic or molecular signals that regulate initial cyst formation in ADPKD may have their origins in this earliest structure of kidney development. ADPKD is a genetically heterozygous disorder that can manifest as cysts in a variety of epithelial organs including liver, pancreas, and kidneys^{45–47}. Although the signs of renal dysfunction typically do not become evident until adulthood, cystogenesis can occur much earlier, with recent evidence pointing to embryonic development⁴⁸. In newborn patients, it has been observed that the rate of cyst formation was maximal during the *in utero* stages of embryonic development⁴⁸. In 85% of ADPKD patients, cyst formation is a result of mutations in the Pkd1 gene, leading to abnormal production and dysregulation of the membrane protein, polycystin, which has been known to play an important role in cell growth, proliferation, migration, and other cellular interactions involved in the structural and functional integrity of the renal tubular epithelium^{49,50}. The expression levels of polycystin-1 during the early phases of nephrogenesis are lower than in the newborn and adult kidneys, indicating that the role of this membrane protein in maintaining tubular architecture may be greater in the postnatal kidney rather than in embryonic stages of

nephron formation. Although the exact mechanism by which dysregulated polycystin-1 contributes to cyst formation is unclear, it is suspected that faulty signaling in the epithelial cells may underlie progressive cystogenesis, which is characterized by the formation of primary dilations in the tubular epithelium, that eventually expand into cavities that are filled with fluid.

Furthermore, it has been noted that even though the primary molecular events that lead to cystogenesis are a result of germline mutations in the PKD genes, this alone is not enough for the full expression of the ADPKD phenotype, suggesting that there might be subsequent secondary disturbances in the synthesis as well as the structural and functional integrity of the polycystin protein which contributes to cystogenesis. A somatic mutation in the normal allele of the Pkd1 gene in conjunction with other cellular events such as increased proliferation, altered planar cell polarity, inflammation, aberrations in extracellular matrix composition, and apoptosis is postulated to be a part of such secondary events that lead to cyst formation^{49,51}. Interestingly, even though the germline mutation of one of the Pkd genes is found in all tubular epithelial cells in human patients with ADPKD, cysts have been

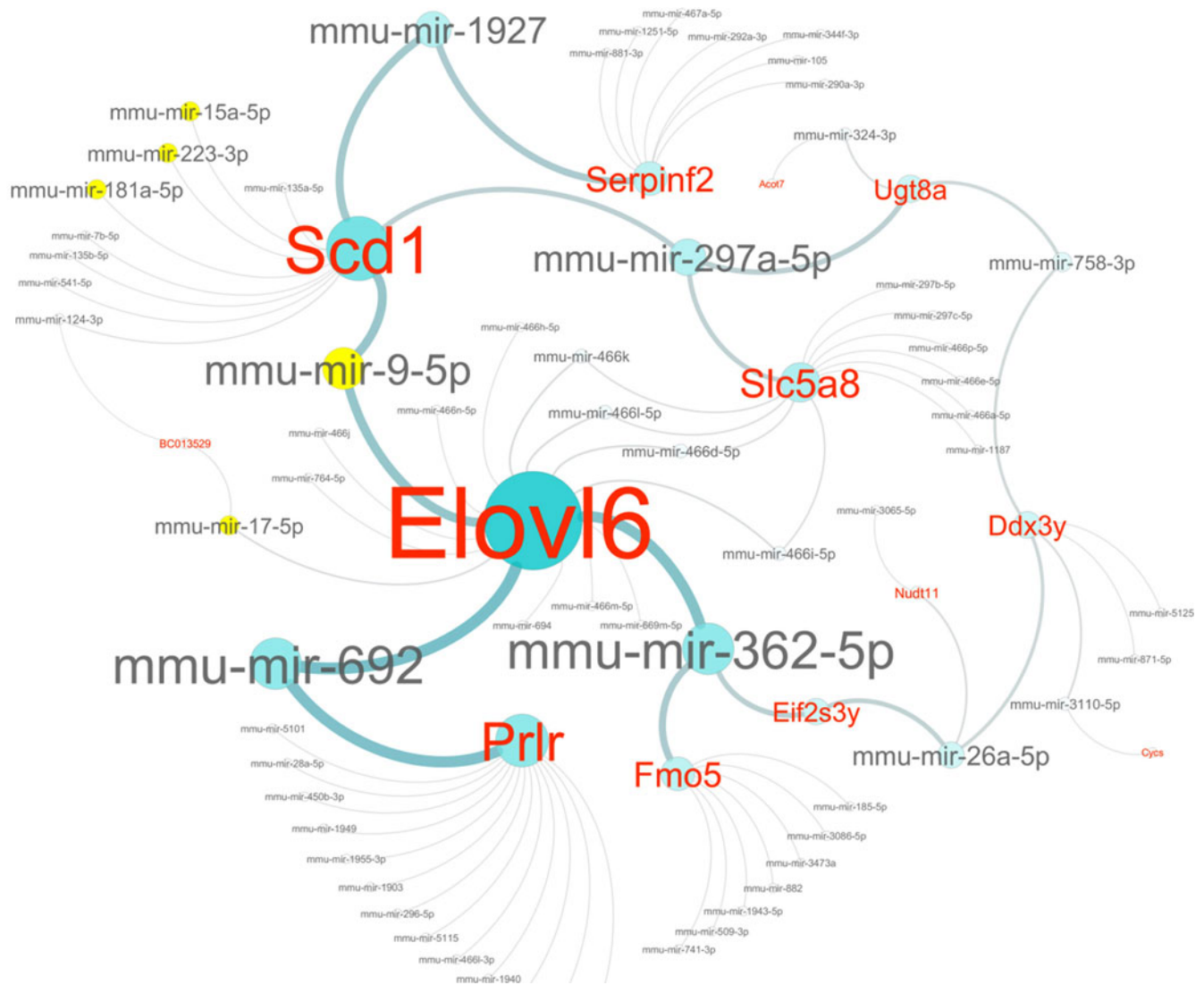


Fig. 4. (Colour online) Network analysis of genes and miRNAs altered in PKD(+/-) kidneys. Using the online tool miRNet, the 267 significantly expressed genes in PKD(+/-) kidneys were used to create a network that specifically focused on miRNAs targeting these genes. Based on these input genes, miRNet generated a network with 138 nodes that included 107 miRNAs and 31 target genes. These nodes were connected by 126 edges that represented biological interactions. Enrichment analysis resulted in further pruning of this network that resulted in 13 subnetworks of varying sizes based on degree of connectivity. The largest network consisted of 78 nodes, 83 edges and included 14 of the input genes that significantly change in the PKD null mouse. This network was analyzed in Cytoscape and redrawn. The nodes labeled in red font are the genes of interest while the rest are various miRNAs that are known to target these genes. The size of the node (and intensity of blue) is directly proportional to its degree of connectivity as expressed in terms of “betweenness centrality”. The miRNAs that have been reported to be associated with PKD are colored in yellow.

observed in only 0.1% of the nephrons, further substantiating the possibility of a second hit in the form of a somatic mutation leading to loss of function in the form of a polycystins. Studies in which *Pkd1* was inactivated in rodents at various time points of prenatal and postnatal kidney development revealed that the inactivation of *Pkd1* at early stages – when the renal tissue is less differentiated – correlated with more severe cystogenesis compared to kidneys with later stage inactivation of *Pkd1*⁵². These studies suggested that the stage of differentiation in the kidney is more crucial in mediating cystogenesis than cell proliferation alone, which indicates that ADPKD disrupts different signaling pathways at different time points during kidney development, making this disease a relatively complex mechanistic problem to tease apart⁵².

In the present study, we demonstrated that the conditional knockout of the *Pkd1* gene in the WD provides a useful experimental model for investigating signaling mechanisms that may underlie the subsequent perturbations in tubular integrity and

function associated with ADPKD. This is the first study to demonstrate that targeted deletion of *Pkd1* in the early embryonic stages of kidney development is sufficient to set the stage for eventual formation of renal cysts, which suggests that the genetic or molecular signals that regulate initial cyst formation in ADPKD may originate in prerenal tissues such as the epithelial WD. Moreover, the viability of the heterozygous *Pkd1*^{+/-}; *Hoxb7-Cre* mutant may make this a useful animal model for further studying the perinatal effects of targeted deletion of the *Pkd1* gene. Although the kidneys of these mice did not exhibit visible cysts in the early postnatal period, the ADPKD phenotype was found to be masking the underlying gene expression in the heterozygous mutant kidneys that were already underway to develop cysts. A variety of signaling pathways that are implicated in tubular function were found to be overrepresented in the genes that showed significant differential expression in the heterozygous mutant kidneys. These pathways mostly included tubular

functions related to metabolism, energetics, xenobiotic biotransformation, and epithelial transport systems.

In addition to changes in gene expression, the present study also investigated miRNAs as potential novel regulatory factors in the embryonic development of cysts in ADPKD. Our bioinformatic analysis predicted several gene–miRNA correlates that have been associated with the polycystic kidney disease phenotype. Analyzing and visualizing this network (Fig. 4) shows that certain genes are targeted by a higher number of miRNAs. For instance, the gene *Elovl6* (involved in elongation of long-chain fatty acids) whose expression is twofold higher in the PKD(+/-) kidneys is predicted to be the target of 15 different miRNAs, of which *mmu-mir-9-5p* and *mmu-mir-17-5p* have been confirmed by the MNDR v2.0 to play a role in PKD^{43,44}. Similarly, *Scd1* (2.8-fold higher expression in PKD(+/-)), which is the second ranking input gene, was found to be targeted by four miRNAs (*mmu-mir-9-5p*, *mmu-mir-15a-5p*, *mmu-mir-223-3p*, and *mmu-mir-181a-5p*) that have also been identified in the MNDR v2.0 database to be associated with PKD. Finer network analysis in Cytoscape allowed for “weighting” the nodes according to centrality, degree of connectedness, and other topological parameters. When ranked according to the node weight (highest to lowest), the input genes could be arranged in the following order: *Elovl6*, *Scd1*, *Prlr*, *Slc5a8*, *Fmo5*, *Serpinf2*, *Ugt8a*, and *Ddx3y*, suggesting that these nodes form critical components of the network underlying the ADPKD phenotype. Similarly, the miRNAs that target these genes were also weighted in the Cytoscape network. Network analysis showed that *mmu-mir-692*, *mmu-mir-362-5p*, and *mmu-mir-9-5p* (all of which were the immediate neighbors for *Elovl6*) were ranked higher in terms of betweenness centrality. Out of these, *mmu-mir-9-5p* has already been established to play a role in ADPKD according to the MNDR v2.0 database.

The results suggest that further studies warrant closer examination of the early WD as a potential source for the genetic signals that regulate ADPKD. The focus of such research would be to next determine whether a direct causal effect can be demonstrated between *Pkd1* and the observed changes gene and miRNA expression in these whole kidneys. Gaining deeper insights into the underlying gene expression signatures and evaluating the signaling networks in association with miRNA components could then lead to targeted experiments to delineate the mechanisms of genetically inherited and embryonically programmed chronic diseases. Such an approach could then potentially lead to markers for earlier detection of ADPKD or gene-based therapies for this disease.

Acknowledgments. We wish to acknowledge the donors and their contributions to the IWK Foundation (Halifax, NS) and Alberta Children’s Hospital Foundation (Calgary, AB), which made this research possible.

Financial Support. This work was supported by both IWK Foundation and Alberta Children’s Hospital Foundation grants (to J.B. Tee). M. Lorenzo was supported by a Markin Undergraduate Student Research Program award from the University of Calgary.

Ethical Standards. All procedures contributing to this work comply with the national ethical standards and guidelines for laboratory animal care and use (Canadian Council on Animal Care, Ottawa, ON) and have been approved by the institutional committees of both the University of Calgary Animal Welfare Committee (protocol M09133, Calgary, AB) and Dalhousie University Committee on Laboratory Animals (protocol 13-045, Halifax, NS).

Author Contributions. All authors contributed to varying degrees on the data analysis and interpretation, drafting, and review of the manuscript.

Conflicts of Interest. The authors declare no conflict of interest.

References

1. NIH Publication No. 10–3895 2010; Available from: <http://kidney.niddk.nih.gov/>.
2. Davies F, Coles GA, Harper PS, Williams AJ, Evans C, Cochlin D. Polycystic kidney disease re-evaluated: a population-based study. *Q J Med.* 1991; 79, 477–485.
3. Tee JB, Acott PD, McLellan DH, Crocker JF. Phenotypic heterogeneity in pediatric autosomal dominant polycystic kidney disease at first presentation: a single-center, 20-year review. *Am J Kidney Dis.* 2004; 43, 296–303.
4. Rossetti S, Consugar MB, Chapman AB, et al. Comprehensive molecular diagnostics in autosomal dominant polycystic kidney disease. *J Am Soc Nephrol.* 2007; 18, 2143–2160.
5. Al-Bhalal L, Akhtar M. Molecular basis of autosomal dominant polycystic kidney disease. *Adv Anat Pathol.* 2005; 12, 126–133.
6. Boletta A, Qian F, Onuchic LF, et al. Polycystin-1, the gene product of PKD1, induces resistance to apoptosis and spontaneous tubulogenesis in MDCK cells. *Mol Cell.* 2000; 6, 1267–1273.
7. Praetorius HA, Frokiaer J, Nielsen S, Spring KR. Bending the primary cilium opens Ca²⁺-sensitive intermediate-conductance K⁺ channels in MDCK cells. *J Membr Biol.* 2003; 191, 193–200.
8. Praetorius HA, Spring KR. Removal of the MDCK cell primary cilium abolishes flow sensing. *J Membr Biol.* 2003; 191, 69–76.
9. Praetorius HA, Spring KR. Bending the MDCK cell primary cilium increases intracellular calcium. *J Membr Biol.* 2001; 184, 71–79.
10. Lin F, Hiesberger T, Cordes K, et al. Kidney-specific inactivation of the KIF3A subunit of kinesin-II inhibits renal ciliogenesis and produces polycystic kidney disease. *Proc Natl Acad Sci U S A.* 2003; 100, 5286–5291.
11. Yoder BK, Hou X, Guay-Woodford LM. The polycystic kidney disease proteins, polycystin-1, polycystin-2, polaris, and cystin, are co-localized in renal cilia. *J Am Soc Nephrol.* 2002; 13, 2508–2516.
12. Pei Y. A “two-hit” model of cystogenesis in autosomal dominant polycystic kidney disease? *Trends Mol Med.* 2001; 7, 151–156.
13. Qian F, Watnick TJ, Onuchic LF, Germino GG. The molecular basis of focal cyst formation in human autosomal dominant polycystic kidney disease type I. *Cell.* 1996; 87, 979–987.
14. Koptides M, Constantinides R, Kyriakides G, et al. Loss of heterozygosity in polycystic kidney disease with a missense mutation in the repeated region of PKD1. *Hum Genet.* 1998; 103, 709–717.
15. Badenas C, Torra R, Perez-Oller L, et al. Loss of heterozygosity in renal and hepatic epithelial cystic cells from ADPKD1 patients. *Eur J Hum Genet.* 2000; 8, 487–492.
16. Ong AC, Harris PC, Davies DR, et al. Polycystin-1 expression in PKD1, early-onset PKD1, and TSC2/PKD1 cystic tissue. *Kidney Int.* 1999; 56, 1324–1333.
17. Lanoix J, D’Agati V, Szabolcs M, Trudel M. Dysregulation of cellular proliferation and apoptosis mediates human autosomal dominant polycystic kidney disease (ADPKD). *Oncogene.* 1996; 13, 1153–1160.
18. Cuellar TL, McManus MT. MicroRNAs and endocrine biology. *J Endocrinol.* 2005; 187, 327–332.
19. Sun W, Julie Li YS, Huang HD, Shyy JY, Chien S. microRNA: a master regulator of cellular processes for bioengineering systems. *Annu Rev Biomed Eng.* 2010; 12, 1–27.
20. Janga SC, Vallabhaneni S. MicroRNAs as post-transcriptional machines and their interplay with cellular networks. *Adv Exp Med Biol.* 2011; 722, 59–74.
21. Lewis BP, Burge CB, Bartel DP. Conserved seed pairing, often flanked by adenosines, indicates that thousands of human genes are microRNA targets. *Cell.* 2005; 120, 15–20.
22. Pandey P, Qin S, Ho J, Zhou J, Kreidberg JA. Systems biology approach to identify transcriptome reprogramming and candidate microRNA targets during the progression of polycystic kidney disease. *BMC Syst Biol.* 2011; 5, 56.
23. Nagalakshmi VK, Ren Q, Pugh MM, Valerius MT, McMahon AP, Yu J. Dicer regulates the development of nephrogenic and ureteric compartments in the mammalian kidney. *Kidney Int.* 2011; 79, 317–330.

24. Pastorelli LM, Wells S, Fray M, *et al.* Genetic analyses reveal a requirement for Dicer1 in the mouse urogenital tract. *Mamm Genome*. 2009; 20, 140–151.
25. Wang E, Hsieh-Li HM, Chiou YY, *et al.* Progressive renal distortion by multiple cysts in transgenic mice expressing artificial microRNAs against Pkd1. *J Pathol*. 2010; 222, 238–248 doi: [10.1002/path.2765](https://doi.org/10.1002/path.2765).
26. Lu W, Peissel B, Babakhanlou H, *et al.* Perinatal lethality with kidney and pancreas defects in mice with a targeted Pkd1 mutation. *Nat Genet*. 1997; 17, 179–181.
27. Arnaout MA. The vasculopathy of autosomal dominant polycystic kidney disease: insights from animal models. *Kidney Int*. 2000; 58, 2599–2610.
28. Kim K, Drummond I, Ibraghimov-Beskrovnyaya O, Klinger K, Arnaout MA. Polycystin 1 is required for the structural integrity of blood vessels. *Proc Natl Acad Sci U S A*. 2000; 97, 1731–1736.
29. Boulter C, Mulroy S, Webb S, Fleming S, Brindle K, Sandford R. Cardiovascular, skeletal, and renal defects in mice with a targeted disruption of the Pkd1 gene. *Proc Natl Acad Sci U S A*. 2001; 98, 12174–12179.
30. Piontek KB, Huso DL, Grinberg A, *et al.* A functional floxed allele of Pkd1 that can be conditionally inactivated in vivo. *J Am Soc Nephrol*. 2004; 15, 3035–3043.
31. Shah MM, Tee JB, Meyer T, *et al.* The instructive role of metanephric mesenchyme in ureteric bud patterning, sculpting, and maturation and its potential ability to buffer ureteric bud branching defects. *Am J Physiol Renal Physiol*. 2009; 297, F1330–F1341.
32. Palsson R, Sharma CP, Kim K, McLaughlin M, Brown D, Arnaout MA. Characterization and cell distribution of polycystin, the product of autosomal dominant polycystic kidney disease gene 1. *Mol Med*. 1996; 2, 702–711.
33. Laboratories J. Mouse strain B6.129S4-Pkd1tm2Ggg/J. 2015; Available from: <http://jaxmice.jax.org/strain/010671.html>.
34. Carroll TJ, Park JS, Hayashi S, Majumdar A, McMahon AP. Wnt9b plays a central role in the regulation of mesenchymal to epithelial transitions underlying organogenesis of the mammalian urogenital system. *Dev Cell*. 2005; 9, 283–292.
35. Kress C, Vogels R, De Graaff W, *et al.* Hox-2.3 upstream sequences mediate lacZ expression in intermediate mesoderm derivatives of transgenic mice. *Development*. 1990; 109, 775–786.
36. Han Y, Chen J, Zhao X, *et al.* MicroRNA expression signatures of bladder cancer revealed by deep sequencing. *PLoS One*. 2011; 6, e18286.
37. Meyer SU, Pfaffl MW, Ulbrich SE. Normalization strategies for microRNA profiling experiments: a 'normal' way to a hidden layer of complexity? *Biotechnol Lett*. 2010; 32, 1777–1788.
38. Mortazavi A, Williams BA, McCue K, Schaeffer L, Wold B. Mapping and quantifying mammalian transcriptomes by RNA-Seq. *Nat Methods*. 2008; 5, 621–628.
39. Fabregat A, Jupe S, Matthews L, *et al.* The reactome pathway knowledge-base. *Nucleic Acids Res*. 2018; 46, D649–D655.
40. Fan Y, Siklenka K, Arora SK, Ribeiro P, Kimmins S, Xia J. miRNet – dissecting miRNA-target interactions and functional associations through network-based visual analysis. *Nucleic Acids Res*. 2016; 44, W135–W141.
41. Garcia-Gonzalez MA, Outeda P, Zhou Q, *et al.* Pkd1 and Pkd2 are required for normal placental development. *PLoS One*. 2010; 5, e12821.
42. Lu W, Shen X, Pavlova A, *et al.* Comparison of Pkd1-targeted mutants reveals that loss of polycystin-1 causes cystogenesis and bone defects. *Hum Mol Genet*. 2001; 10, 2385–2396.
43. Wang Y, Chen L, Chen B, *et al.* Mammalian ncRNA-disease repository: a global view of ncRNA-mediated disease network. *Cell Death Dis*. 2013; 4, e765.
44. Cui T, Zhang L, Huang Y, *et al.* MNDR v2.0: an updated resource of ncRNA-disease associations in mammals. *Nucleic Acids Res*. 2018; 46, D371–D374.
45. Gabow PA. Autosomal dominant polycystic kidney disease. *N Engl J Med*. 1993; 329, 332–342.
46. Reed BY, McFann K, Bekheirnia MR, *et al.* Variation in age at ESRD in autosomal dominant polycystic kidney disease. *Am J Kidney Dis*. 2008; 51, 173–183.
47. Shamshirsaz AA, Reza Bekheirnia M, Kamgar M, *et al.* Autosomal-dominant polycystic kidney disease in infancy and childhood: progression and outcome. *Kidney Int*. 2005; 68, 2218–2224.
48. Grantham JJ, Cook LT, Wetzel LH, Cadnapaphornchai MA, Bae KT. Evidence of extraordinary growth in the progressive enlargement of renal cysts. *Clin J Am Soc Nephrol*. 2010; 5, 889–896.
49. Igarashi P, Somlo S. Genetics and pathogenesis of polycystic kidney disease. *J Am Soc Nephrol*. 2002; 13, 2384–2398.
50. Torres VE, Harris PC, Pirson Y. Autosomal dominant polycystic kidney disease. *Lancet*. 2007; 369, 1287–1301.
51. Zhou J. Polycystins and primary cilia: primers for cell cycle progression. *Annu Rev Physiol*. 2009; 71, 83–113.
52. Piontek K, Menezes LF, Garcia-Gonzalez MA, Huso DL, Germino GG. A critical developmental switch defines the kinetics of kidney cyst formation after loss of Pkd1. *Nat Med*. 2007; 13, 1490–1495.